### **OPEN ACCESS**



# Lagrangian Stochastic Model for the Motions of Magnetic Footpoints on the Solar Wind Source Surface and the Path Lengths of Boundary-driven Interplanetary Magnetic Field Lines

Gang Li and N. H. Bian

Department of Space Science, University of Alabama in Huntsville, Huntsville, AL, 35899, USA; gangli.uah@gmail.com Received 2023 January 3; revised 2023 February 14; accepted 2023 February 16; published 2023 March 16

## **Abstract**

In this work, we extend Leighton's diffusion model describing the turbulent mixing of magnetic footpoints on the solar wind source surface. The present Lagrangian stochastic model is based on the spherical Ornstein–Uhlenbeck process with drift that is controlled by the rotation frequency  $\Omega$  of the Sun, the Lagrangian integral timescale  $\tau_{\rm L}$ , and the root-mean-square footpoint velocity  $V_{\rm rms}$ . The Lagrangian velocity and the positions of magnetic footpoints on the solar wind source surface are obtained from the solutions of a set of stochastic differential equations, which are solved numerically. The spherical diffusion model of Leighton is recovered in the singular Markov limit when the Lagrangian integral timescale tends to zero while keeping the footpoint diffusivity finite. In contrast to the magnetic field lines driven by standard Brownian processes on the solar wind source surface, the interplanetary magnetic field lines are smooth differentiable functions with finite path lengths in our model. The path lengths of the boundary-driven interplanetary magnetic field lines and their probability distributions at 1 au are computed numerically, and their dependency with respect to the controlling parameters is investigated. The path-length distributions are shown to develop a significant skewness as the width of the distributions increases.

Unified Astronomy Thesaurus concepts: Interplanetary turbulence (830); Interplanetary magnetic fields (824)

### 1. Introduction

The interplanetary magnetic field is an essential component of the solar-terrestrial connections. The structure of the solar wind magnetic field is critical to the understanding of solar energetic particle (SEP) events. In the original work of Parker (1958), the magnetic field is carried radially outward with the bulk solar wind that emanates from the rotating Sun as a whole. This yields the basic spiral structure of the interplanetary magnetic field lines. Soon after the first diagnosis of turbulence in the solar wind, Jokipii & Parker (1969) pointed out the importance of random fluctuations in astrophysical magnetic fields. On the basis of the Leighton (1964) theory of diffusive flux transfer on the photosphere, Jokipii & Parker (1969) argued that the Parker spirals are stochastic, providing a sound explanation to the longitudinal spread of high-energy particles released at the Sun. Stochastic Parker spirals in the solar wind can be represented well by realizations of a spherical Brownian diffusion process superimposed on the angular drift due to the solar rotation (Bian & Li 2021). In this picture, multiple field lines traced back to the Sun from the observer position can magnetically connect to different locations on the source surface, although with different probabilities. The resulting longitudinal spread of interplanetary magnetic field lines and of SEPs can be described by the circular Gaussian distribution (Bian & Li 2022a). After the pioneering investigations by Fan et al. (1968), the angular spread of SEPs has been the subject of detailed spacecraft measurements, in both longitude (Van Hollebeke et al. 1975; Cane et al. 1986; Shea & Smart 1990; Reames 1999; Lario et al. 2006; Mewaldt et al. 2013;

Original content from this work may be used under the terms of the Creative Commons Attribution 4.0 licence. Any further distribution of this work must maintain attribution to the author(s) and the title of the work, journal citation and DOI.

Wiedenbeck et al. 2013; Reames et al. 2013; Dresing et al. 2014; Richardson et al. 2014; Cohen et al. 2017) and latitude (Zhang et al. 2001, 2003; Dalla et al. 2003). The multipoint statistical study realized by Cohen et al. (2017) reveals that the width of the longitudinal distributions of ions only weakly depends on the charge to mass ratio. It is suggestive that the angular spread of SEPs relies on processes that are similar to those responsible for the dispersion of magnetic field lines in the solar wind.

An extension of the Jokipii & Parker (1969) models was presented by Giacalone & Jokipii (2004) (see also Giacalone 2001). In the Giacalone & Jokipii (2004) model, the motions of footpoints are prescribed by the Eulerian surface velocity field, which is derived from a spherical stream function on the source surface. The weighting coefficients in the spherical harmonic decomposition of the stream function can be constrained from observations of the Eulerian spectrum of photospheric convection (Hathaway et al. 2000, 2015; Rincon et al. 2017; Rincon & Rieutord 2018). Giacalone & Jokipii (2004) performed numerical integration of the footpoint trajectories and compared the spatial distribution of footpoints with the solution of a spherical diffusion equation, yielding values of the footpoint diffusivity  $\sim 1500-2000 \,\mathrm{km^2 s^{-1}}$  close to those inferred by Leighton (1964). The boundary-driven model of Giacalone & Jokipii (2004) has also formed the basis of several studies investigating how stochastic magnetic field lines impact the interplanetary transport of SEPs (Pei et al. 2006; Kelly et al. 2012; Moradi & Li 2019). In this work, we present a Lagrangian stochastic model describing the turbulent motions of the magnetic footpoints. Our model is a direct extension of the Leighton (1964)s diffusion model. It is a model for the Lagrangian surface velocity on the solar wind source surface.

Turbulent magnetic field fluctuations in the solar wind are expected to affect not only the magnetic connection angles but also the connection lengths, in particular for SEP events showing large angular spreads. The connection lengths, which are the distances traveled by the particles, can be inferred from the velocity dispersion analysis of SEP events (Lin 1974; Lin et al. 1981; Krucker & Lin 2000; Tylka et al. 2003; Sáiz et al. 2005; Kahler & Ragot 2006; Reames 2009; Wang et al. 2016) and also from the fractional velocity dispersion analysis recently proposed by Zhao et al. (2019). Using recent observations from the IS⊙IS instrument on board the Parker Solar Probe spacecraft, Chhiber et al. (2021) examined how the random walk of magnetic field lines in the solar wind can affect the SEP path lengths.

In Section 2, we formulate the Lagrangian stochastic model extending the Leighton (1964)s model for magnetic flux diffusion on the photosphere. The results are used in Section 3 to extend the Jokipii & Parker (1969) model of surface-driven magnetic field lines in the heliosphere. A summary and conclusions are given in Section 4.

# 2. Generalized Leighton's Model for the Motions of Magnetic Footpoints

The solar wind source surface denotes the inner boundary of the solar wind magnetic field. It is the outer boundary of the coronal magnetic field. In the solar corona, magnetic field lines are an admixture of closed and open field lines all originating from a common inner boundary: the solar photosphere. Potential Field Source Surface models (Schatten et al. 1969; Altschuler & Newkirk 1969; Schrijver & DeRosa 2003; Gombosi et al. 2018) are commonly used to describe the magnetic field expansion from the photosphere to the source surface. In this work, we are not concerned with the coronal expansion of the magnetic field and hence with the exact location of the solar wind source surface. It can be chosen to coincide with the location adopted in PFFS models or taken as the location of the Alfvén critical surface predicted by DeForest et al. (2014) and Adhikari et al. (2019), beyond which the solar wind becomes super-Alfvénic. The magnetic footpoint trajectories on the solar wind source surface can be described by the solutions of the equation

$$\frac{d\mathbf{r}_{\perp}(t)}{dt} = \mathbf{V}_{\perp}(\mathbf{r}_{\perp}, t),\tag{1}$$

where  $V_{\perp}(r_{\perp}, t)$  is the surface velocity field, a function of the position  $r_{\perp}$  on the source surface and on time t. The position  $r_{\perp}(t)$  of the magnetic footpoints remains on a sphere, and hence,  $|r_{\perp}(t)| = r_0$  at all times. The velocity  $V_{\perp}(r_{\perp}, t)$  appearing in Equation (1) is the Eulerian surface velocity field everywhere tangent to the source surface. Let us decompose this velocity field into a mean component resulting from rigid body rotation plus turbulent fluctuations as

$$V_{\perp}(\mathbf{r}_{\perp}, t) = V_{\Omega}(\mathbf{r}_{\perp}) + \delta V_{\perp}(\mathbf{r}_{\perp}, t). \tag{2}$$

In the reduced heliographic coordinate system  $(r = r_0, \theta, \phi)$ , where  $\theta$  is the latitude and  $\phi$  is the longitude, the secular rotation velocity of the footpoints is given by  $V_{\Omega} = \Omega r_0 \sin \theta u_{\phi}$ , where  $\Omega$  is the solar rotation frequency. Expressed in this

coordinate system, Equation (1) takes the form

$$\frac{d\theta(t)}{dt} = \frac{\delta V_{\theta}(\theta, \phi, t)}{r_0}, \qquad \frac{d\phi(t)}{dt} = \Omega + \frac{\delta V_{\phi}(\theta, \phi, t)}{r_0 \sin \theta}.$$
 (3)

There are three fundamental parameters associated with the turbulent component  $\delta V_{\perp}(r_{\perp}, t)$  of the Eulerian velocity field. These parameters are the typical amplitude of the fluctuations  $V_{\rm rms}$ , the correlation length  $\lambda_c = \Theta_c r_0$ , where  $\Theta_c$  represents the typical angular size of source surface convective structures, and the correlation time  $\tau_c$ , which represents the lifetime of these structures. Assuming the Eulerian velocity field  $\delta V_{\perp}({\it r}_{\perp},{\it t})$  is a Gaussian, homogeneous, stationary, and isotropic random vector field on the sphere, then the set of parameters  $(\Omega, V_{\rm rms}, \Theta_c, \text{ and } \tau_c)$  fully determine the statistical properties of the footpoint trajectories on the solar wind source surface. It can easily be shown that the turbulent part of the footpoint motion, describing the deviations  $\delta r_{\perp}(t)$  from rigid body rotation, is solely controlled by the dimensionless Kubo number,  $K = \tau_c V_{\rm rms}/\Theta_c r_0$ , which represents the typical lifetime  $au_{\rm c}$  of convective structures in units of the turnover time  $\lambda_{\rm c}/V_{\rm rms}$  of footpoints convected by such structures. The parameters  $\lambda_c$  and  $V_{\rm rms}$  of the Eulerian surface velocity field can be constrained from high-resolution spectroscopic imaging of the Doppler field (Hathaway et al. 1996; Hathaway & Rightmire 2010).

On the other hand, the properties of the Lagrangian surface velocity  $V_{\perp}(t)$  can be established, for instance, by recording the position of identifiable moving features as a function of time on the surface of the Sun (Van Kooten & Cranmer 2017). Adopting a Lagrangian perspective, Bian & Li (2022b) have recently described the local structure of stochastic Parker spirals resulting from in situ turbulence in the solar wind. The approach adopted by Bian & Li (2022b) affords a resolution to the long-standing conundrum that magnetic field lines undergoing a heliospheric Brownian diffusion are nowhere differentiable and therefore have infinite path lengths. Our current problem concerns the effects of source surface turbulence on the interplanetary magnetic field lines, and we shall here also base our modeling approach on a Lagrangian perspective. The Lagrangian velocity  $V_{\perp}(t)$  of the magnetic footpoints is related to the Eulerian velocity field  $V_{\perp}(r_{\perp}, t)$  on the solar wind source surface by

$$V_{\perp}(t) = \int V_{\perp}(\mathbf{r}_{\perp}, t) \, \delta(\mathbf{r}_{\perp} - \mathbf{r}_{\perp}(t)) d\mathbf{r}_{\perp}, \tag{4}$$

where  $r_{\perp}(t)$  is the solution of Equation (1). In other words, the Lagrangian velocity  $V_{\perp}(t) = V_{\perp}(r_{\perp}(t), t)$  of magnetic footpoints, which is a function of time only, is the Eulerian velocity evaluated along the footpoint trajectories. The Lagrangian integral timescale  $\tau_L$  is defined via the relation

$$\lim_{t \to \infty} \int_0^t \langle \delta V_{\perp}(0) \cdot \delta V_{\perp}(\tau) \rangle d\tau = \tau_{\rm L} V_{\rm rms}^2.$$
 (5)

Note that the Eulerian correlation time  $\tau_c$  and the Lagrangian correlation time  $\tau_L$  are fundamentally different characteristic timescales. The time integral involved in Equation (5) has the physical dimension of a diffusivity (cm<sup>2</sup> s<sup>-1</sup>), and it converges

toward a constant, provided the Lagrangian autocorrelation function  $\langle \delta V_\perp(0) \cdot \delta V_\perp(\tau) \rangle$  decays sufficiently fast. This constant, denoted here by  $\kappa = \tau_L V_{\rm rms}^2$ , is by definition the spatial diffusivity of the magnetic footpoints. Indeed, from the footpoint equation of motion (1), one can derive Taylor's relation,

$$\frac{1}{2} \frac{d \left\langle \delta r_{\perp}^{2}(t) \right\rangle}{dt} = \int_{0}^{t} \left\langle \delta \mathbf{V}_{\perp}(0) \cdot \delta \mathbf{V}_{\perp}(\tau) \right\rangle d\tau, \tag{6}$$

which is an exact result connecting the footpoint displacements variance  $\langle \delta r_{\perp}^2(t) \rangle$  and the Lagrangian autocorrelation function  $\langle \delta V_{\perp}(0) \cdot \delta V_{\perp}(\tau) \rangle$ , the trace of the Lagrangian autocorrelation tensor. In the limit when  $t \gg \tau_L$ , Equation (6) yields the diffusive behavior  $\langle \delta r_{\perp}^2(t) \rangle = 2\tau_L V_{\rm rms}^2 t$ . However, when  $t \ll \tau_L$ , Equation (6) gives  $\langle \delta r_{\perp}^2(t) \rangle = V_{\rm rms}^2 t^2$ , indicating that the footpoint trajectories are linear functions of time for time intervals much smaller than the integral timescale  $\tau_L$ . Assuming, as in Leighton (1964), that the magnetic field footpoints undergo a Brownian diffusion at all times, their trajectories obey the drift–diffusion equations given by

$$\frac{d\mathbf{r}_{\perp}(t)}{dt} = \mathbf{V}_{\Omega} + \sqrt{\tau_L V_{\rm rms}^2} \boldsymbol{\zeta}(t), \tag{7}$$

where  $\zeta(t)$  is the two-dimensional unit Gaussian white noise having the following properties:

$$\langle \zeta_i(t) \rangle = 0, \qquad \langle \zeta_i(t) \zeta_j(t') \rangle = \delta_{ij} \delta(t - t').$$
 (8)

Therefore, in the Leighton (1964) model, the Lagrangian surface velocity, which coincides with the velocity of the magnetic footpoints, is modeled by the Gaussian white noise process. A natural extension of the Leighton (1964) diffusion model consists in modeling the turbulent component of the Lagrangian surface velocity by a Gaussian process whose autocorrelation function decays exponentially on a timescale  $\tau_L$ :

$$\langle \delta V_{\perp}(t) \cdot \delta V_{\perp}(0) \rangle = V_{\rm rms}^2 e^{-\frac{t}{\tau_L}}.$$
 (9)

The footpoint trajectories on the solar wind source surface thus satisfy the equations:

$$\frac{d\mathbf{r}_{\perp}(t)}{dt} = \mathbf{V}_{\Omega} + \delta \mathbf{V}_{\perp}(t), 
\frac{d\delta \mathbf{V}_{\perp}(t)}{dt} = -\frac{\delta \mathbf{V}_{\perp}(t)}{\tau_{L}} + \sqrt{\frac{\mathbf{V}_{\text{rms}}^{2}}{\tau_{L}}} \boldsymbol{\zeta}(t). \tag{10}$$

The second equation above, which is the Langevin equation, can be rewritten in a compact dimensionless form as

$$\frac{d\delta \tilde{\mathbf{V}}_{\perp}(\tilde{t})}{d\tilde{t}} = -\delta \tilde{\mathbf{V}}_{\perp}(\tilde{t}) + \boldsymbol{\zeta}(\tilde{t}), \tag{11}$$

where  $\delta \tilde{V}_{\perp} = \delta V_{\perp}/V_{\rm rms}$  and  $\tilde{t} = t/\tau_L$ . Note that taking the limit  $\tau_L \to 0$  while keeping the product  $\tau_L V_{\rm rms}^2 = \kappa$  finite in Equation (10) recovers Leighton's diffusive prescription:

 $\delta V_{\perp}(t) = \sqrt{ au_L V_{
m rms}^2} \, \zeta(t)$ . Equation (10) can be integrated to give  $\delta V_{\perp}(t) = \delta V_{\perp}(0)e^{-t/\tau_L} + \sqrt{\tau_L V_{\rm rms}^2} \int_0^t e^{-(t-t')/\tau_L} \boldsymbol{\zeta}(t') dt',$ and hence,  $\langle (\delta V_{\perp}(t) - \delta V_{\perp}(0)e^{-t/\tau_L})^2 \rangle = V_{\text{rms}}^2(1 - e^{-2t/\tau_L})$  $ightarrow V_{
m rms}^2$  when  $t\gg au_L$ . The deviation from solid body rotation  $\delta r_{\perp}(t) = \int_0^t \delta V_{\perp}(t') dt'$  is a non-Markovian process that can be expressed as a linear combination of Brownian motions weighted by an exponential kernel, superimposed on the contribution due to initial conditions, as  $\delta \mathbf{r}_{\perp}(t) =$  $\delta V_{\perp}(0) \tau_L (1 - e^{-t/\tau_L}) + \sqrt{\tau_L V_{\rm rms}^2} \int_0^t (1 - e^{-(t-t')/\tau_L}) dW_{t'},$ where  $W_t$  denotes the Wiener process. The footpoint trajectories given by Equation (10) are the integrals of a continuous stochastic process: the Ornstein-Uhlenbeck process. They are thus random functions of time, but nevertheless they remain differentiable. The spatial distribution  $P(r_{\perp}, t)$  of magnetic footpoints is the Gaussian distribution whose variance is given by

$$\langle \delta r_{\perp}^2(t) \rangle = 2\tau_L V_{\rm rms}^2 [t + \tau_L (e^{-\frac{t}{\tau_L}} - 1)], \tag{12}$$

which satisfies the two asymptotic constraints imposed by the Taylor relation (6).

In order to formulate the Lagrangian stochastic model globally describing the footpoint motions on the spherical source surface, we can use the following finite difference scheme:  $\mathbf{r}_{\perp}(t+\Delta t)=\mathbf{r}_{\perp}(t)+(V_{\Omega}+\delta V_{\perp}(t))\Delta t, \delta V_{\perp}(t+\Delta t)=\delta V^D(t)[1-(\Delta t/\tau_L)]+\sqrt{V_{\rm rms}^2(\Delta t/\tau_L)}\,\boldsymbol{\zeta}$ , where  $\boldsymbol{\zeta}$  is a two-dimensional centered Gaussian random number with unit variance drawn from independent identical distributions at each time step  $\Delta t$  and  $\delta V^D(t)$  is the turbulent component of the footpoint velocity dragged to  $\mathbf{r}_{\perp}(t+\Delta t)$ . Therefore, in the reduced heliographic coordinate system, with  $\mathbf{u}_{\theta}$  and  $\mathbf{u}_{\phi}$  as the unit tangent vectors forming an orthonormal basis, the finite difference formulation of Equation (10) takes the form:

$$\phi(t + \Delta t) = \phi(t) + \left(\Omega + \frac{\delta V_{\phi}(t)}{r_{0} \sin \theta(t)}\right) \Delta t,$$

$$\theta(t + \Delta t) = \theta(t) + \frac{\delta V_{\theta}(t)}{r_{0}} \Delta t,$$

$$\delta V_{\theta}(t + \Delta t) = \delta V_{\theta}(t) (1 - \frac{\Delta t}{\tau_{L}}) + \delta V_{\phi}(t) \cos \theta(t)$$

$$\times \left(\Omega + \frac{\delta V_{\phi}(t)}{r_{0} \sin \theta(t)}\right) \Delta t + \sqrt{V_{\text{rms}}^{2} \left(\frac{\Delta t}{\tau_{L}}\right)} \zeta_{\theta}$$

$$\delta V_{\phi}(t + \Delta t) = \delta V_{\phi}(t) (1 - \frac{\Delta t}{\tau}) - \delta V_{\theta}(t) \cos \theta(t)$$

$$\times \left(\Omega + \frac{\delta V_{\phi}(t)}{r_{0} \sin \theta(t)}\right) \Delta t + \sqrt{V_{\text{rms}}^{2} \left(\frac{\Delta t}{\tau_{L}}\right)} \zeta_{\phi}.$$
(13)

The Lagrangian stochastic model given by Equation (13) describes the trajectories of the magnetic footpoints on the spherical solar wind source surface of radius  $r_0$ , taken here at 2.5 solar radii. The turbulent component of the magnetic footpoint motion is controlled by the two-parameter doublet  $(\tau_L, V_{rms})$ . Five different realizations of magnetic footpoint trajectories  $[\theta(t), \phi(t)]$  on the source surface, obtained by numerical integration of Equation (13), are plotted in Figure 1.

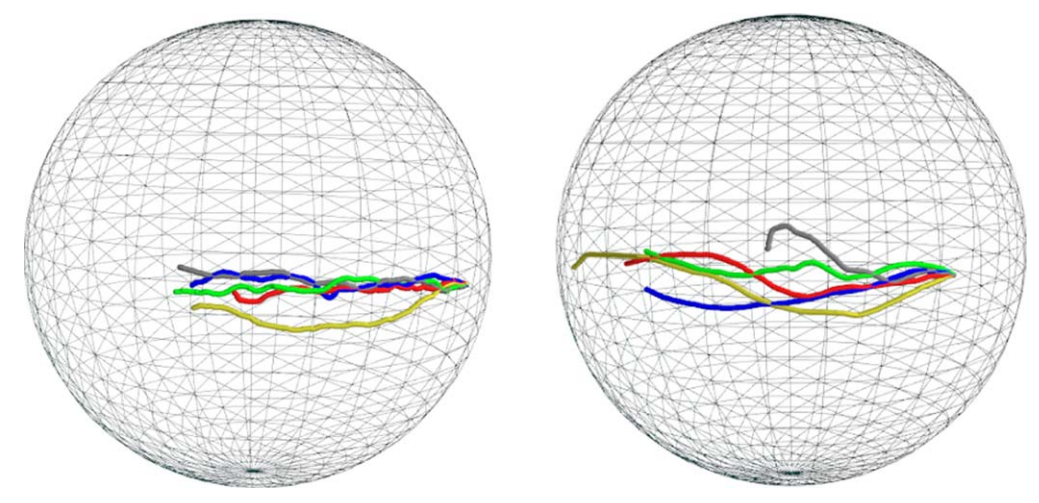
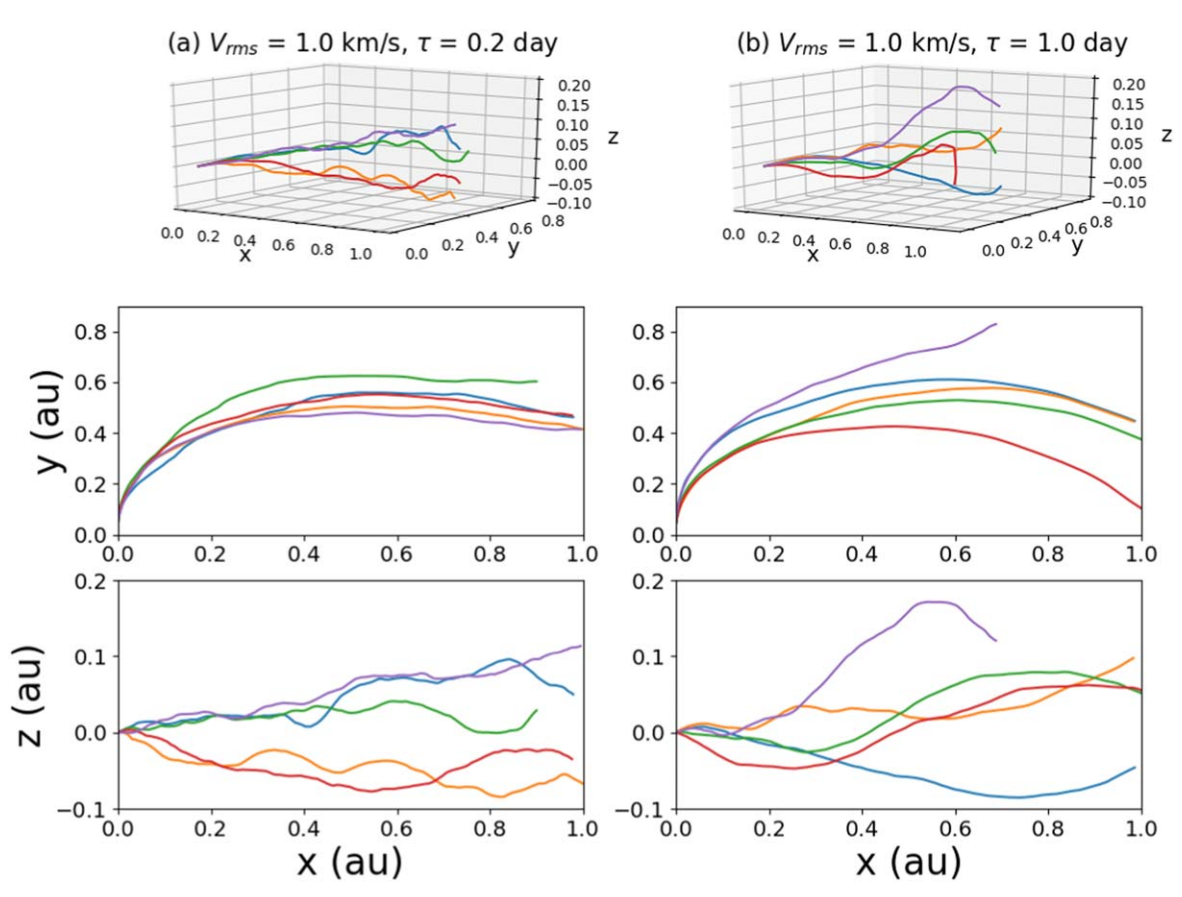


Figure 1. Five realizations of footpoint trajectories on the source surface  $r = r_0$  resulting from the numerical integration of Equation (13). In both panels,  $V_{\rm rms} = 1$  km s<sup>-1</sup>, while  $\tau_L = 0.2$  day in the left panel and  $\tau_L = 1.0$  day in the right panel.



**Figure 2.** Top: five realizations of boundary-driven solar wind magnetic field lines corresponding to the footpoint trajectories displayed in Figure 1. Middle: their projections into the XY plane. Bottom: their projections into the XZ plane.

In both panels,  $V_{\rm rms}=1.0~{\rm km~s}^{-1}$ , with  $\tau_L=0.2~(1.0)$  day in the left (right) panel. We observe that increasing the Lagrangian autocorrelation time  $\tau_L$  results in smoother footpoint trajectories and larger angular spread.

# 3. The Path Lengths of Boundary-driven Interplanetary Magnetic Field Lines

Due to the very high electrical conductivity of the solar wind plasma, the magnetic field can be considered to be frozen in the solar wind, and hence each source surface-driven magnetic field line is determined by the position of fluid elements continuously ejected over time by the solar wind from a given moving magnetic footpoint. Therefore, the solar wind velocity, which is assumed here to be purely radial and equal to a constant  $V_{\rm sw} = 400~{\rm km~s}^{-1}$ , provides a one-to-one map between the footpoint trajectories  $[\theta(t), \phi(t)]$  on the source surface and the boundary-driven magnetic field lines  $[r(t) = r_0 + V_{\rm sw} \ t, \ \theta(t), \ \phi(t)]$  in the heliosphere, which are here parameterized by t. The boundary-driven magnetic field lines corresponding to the turbulent footpoint trajectories displayed

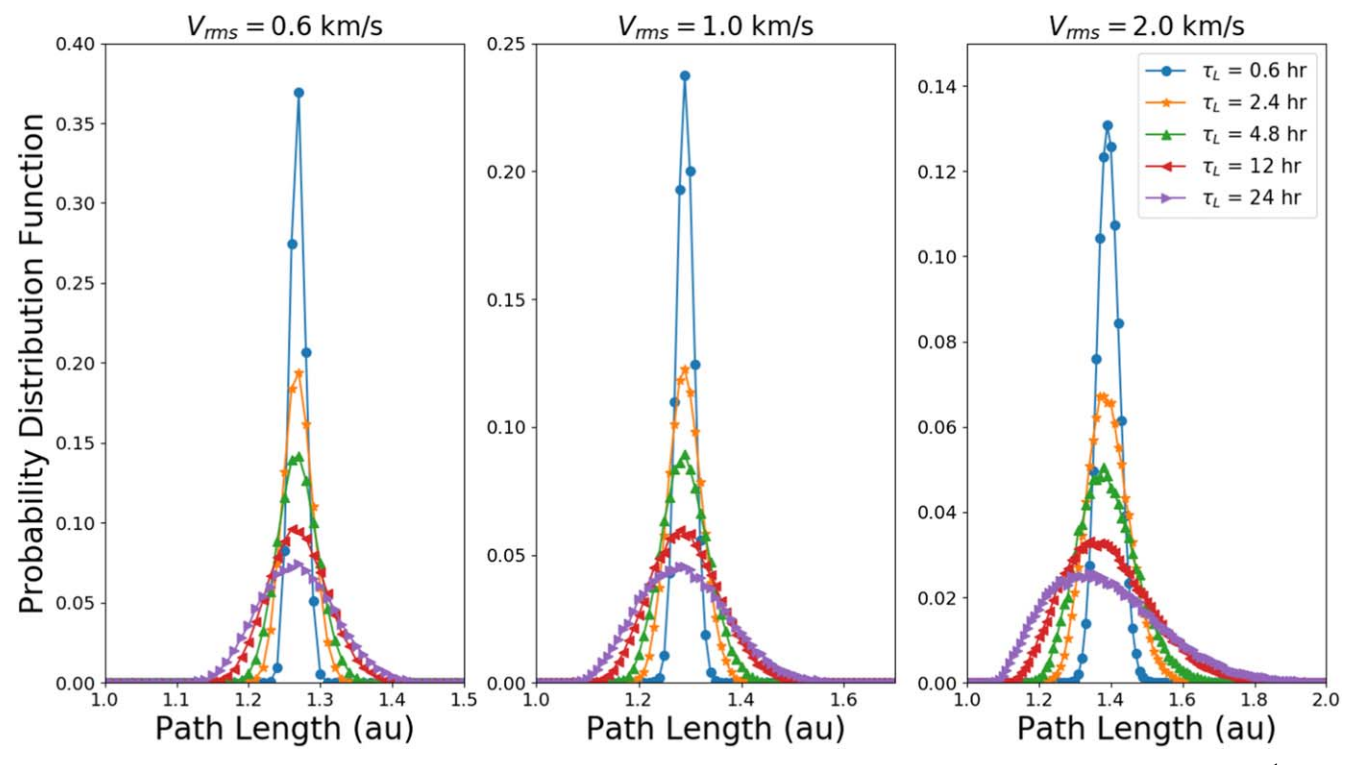


Figure 3. The probofability distribution function P(L, r = 1 au) of the magnetic path length L at 1 au. The left panel corresponds to  $V_{\rm rms} = 0.6 \text{ km. s}^{-1}$  at the solar surface, the middle panel to  $V_{\rm rms} = 1.0 \text{ km s}^{-1}$ , and the right panel to  $V_{\rm rms} = 2.0 \text{ km} \cdot \text{s}^{-1}$ .

in Figure 1 are plotted in Figure 2. The two upper panels are representations of the magnetic field lines in three dimensions, the two middle panels are projections of the field lines into the XY plane, and the two lower panels are projections of the field lines into the XZ plane.

While these field lines are stochastic, they are smooth differentiable functions of r (or t). Their path length L(r) from the source surface to an observer located at a distance r is thus a well-defined random function of r given by

$$L(r) = \int_0^{r/V_{\text{sw}}} dt \sqrt{V_{\text{sw}}^2 + r^2(t) \left(\frac{d\theta(t)}{dt}\right)^2 + r^2(t) \sin^2 \theta(t) \left(\frac{d\phi(t)}{dt}\right)^2},$$
(14)

where  $r(t) = r_0 + V_{sw} t$ . It should be noted that we ignored the effects of in situ turbulence resulting in the motions of the solar wind parcels perpendicular to the background field. Inclusion of such effects will be examined in a future paper. The probability distribution functions P(L, r = 1 au) of the magnetic connection length L at the distance r = 1au are plotted in Figure 3. The nominal Parker field line length is  $L_0 \simeq 1.17$  au at 1 au. The rms speed  $V_{\rm rms}$  is equal to 0.6, 1.0, and 2.0 km s<sup>-1</sup> in the left, middle, and right panels, respectively. In each panel, the PDFs are plotted for five different values of the Lagrangian integral timescale  $\tau_L$ : 0.6, 2.4, 4.8, 12, and 24 hr, which are labeled by different colors. The deviations from Gaussian-like distributions increase as the width of the PDFs increases and the positive skewness becomes more pronounced. From the N realizations of the stochastic magnetic field lines, we compute the average  $\bar{L}$ , the standard deviation  $\sigma$ , and the skewness  $\tilde{\mu}_3$ ,

**Table 1** The Average Length  $\bar{L}$ , the Standard Deviation  $\sigma$ , Both in Astronomical Units, and the Skewness  $\tilde{\mu}_3$  (Dimensionless) Corresponding to the PDFs in Figure 3

$\overline{\tau_L}$ (hr)	$V_{ m rms} = 0.6~{ m km~s^{-1}}$ $\bar{L},~\sigma,~\tilde{\mu}_3$	$V_{ m rms} = 1.0~{ m km~s^{-1}}$ $\bar{L},~\sigma,~\tilde{\mu}_3$	$V_{\rm rms} = 2.0~{\rm km~s}^{-1}$ $\bar{L},~\sigma,~\tilde{\mu}_3$
0.6	1.27, 0.01, 0.04	1.30, 0.02, 0.08	1.40, 0.03, 0.15
2.4	1.27, 0.02, 0.09	1.30, 0.03, 0.16	1.40, 0.06, 0.31
4.8	1.27, 0.03, 0.12	1.30, 0.05, 0.21	1.40, 0.08, 0.41
12	1.27, 0.04, 0.17	1.30, 0.07, 0.30	1.40, 0.12, 0.57
24	1.27, 0.05, 0.20	1.30, 0.09, 0.33	1.40, 0.16, 0.63

given by

$$\bar{L} = \frac{1}{N} \sum_{i} L_{i}, \qquad \sigma = \sqrt{\frac{1}{N}} \sum_{i} (L_{i} - \bar{L})^{2},$$

$$\tilde{\mu}_{3} = \frac{1}{N} \sum_{i} \left( \frac{(L_{i} - \bar{L})}{\sigma} \right)^{3}, \qquad (15)$$

of each path-length distribution. These three quantities are compiled in Table 1. As we can see from the table, as  $\tau_L$  increases at fixed  $V_{\rm rms}$ , the average path length remains the same while the standard deviation and skewness increase. For the case of  $V_{\rm rms}=1.0~{\rm km~s^{-1}}$  in the middle panel, the PDFs are similar to the cases of  $V_{\rm rms}=0.6~{\rm km~s^{-1}}$  with  $\bar{L}=1.3~{\rm au}$  for all five values of  $\tau_L$  and larger standard deviation and skewness. For fixed  $\tau_L$ , the skewness is the largest when the speed  $V_{\rm rms}$  is the largest, here  $V_{\rm rms}=2.0~{\rm km~s^{-1}}$ . For fixed  $V_{\rm rms}$ , the skewness is the largest when the decorrelation time  $\tau_L$ 

is the largest, here  $\tau_L=24\,\mathrm{hr}$ . This is expected because the standard deviation  $\sigma$  of the path length distribution increases with the footpoint diffusivity  $\kappa=\tau_L V_{\mathrm{rms}}^2$ . A large  $\sigma$  implies a large skewness  $\tilde{\mu}_3$ , because the distribution of L is positive (indeed L>1 au) and the mean  $\bar{L}$  remains almost constant. It should be noted that, when the diffusivity is increased, there are more realizations of magnetic field lines with path lengths smaller than 1.2 au, the nominal Parker field path length.

The path-length distributions shown in Figure 3 share some similarities with those obtained earlier by Moradi & Li (2019) based on the Eulerian model of Giacalone (2001) and Giacalone & Jokipii (2004), where the surface stream function is decomposed into a sum of spherical harmonics. The amplitudes of the different spherical harmonic modes (l,m) in this model are constrained by observations of the supergranular component of the photospheric convection spectrum. There are three controlling parameters in this Eulerian model: the rms speed  $V_{\rm rms}$ ; the Eulerian correlation timescale  $\tau_c$ ; and  $l_{\text{max}}$ , which represents the highest wavenumber in the spherical harmonic decomposition. The wavenumber  $l_{\text{max}}$  corresponds to the smallest resolved angular scale of the stream function in Giacalone (2001) and Moradi & Li (2019), which is  $\sim 2\pi/l_{\text{max}}$ . The Eulerian timescale  $\tau_c$  considered in Giacalone (2001) and Moradi & Li (2019) represents the typical lifetime of supergranular convective cells, with the latter being much less accurately constrained from Doppler measurements than are  $V_{\rm rms}$  and  $\lambda_c$ . In comparison, the turbulent part of the present Lagrangian stochastic model is governed by the rms speed  $V_{\rm rms}$  and the Lagrangian autocorrelation time  $\tau_L$ . By construction, there is no explicit spatial scale similar to  $\lambda_c$  entering as a control parameter in the present Lagrangian stochastic model given by Equation (13). We finally observe that, while the introduction of a stream function in the Eulerian model of Giacalone (2001) and Giacalone & Jokipii (2004) relies on the assumption of incompressible surface flows on the photosphere, the Leighton (1964) model and its generalization presented in this work do not require such a hypothesis.

### 4. Summary and Conclusions

Leighton (1964) introduced a zeroth-order Lagrangian stochastic model describing turbulent mixing on the photosphere, which is the spherical analog of the Brownian motion superimposed on the secular drift due to the solar rotation. In the heliographic coordinate system, the stochastic formulation of the Leighton (1964) spherical drift-diffusion equation is (Bian & Li 2021)

$$r_0 \frac{d\theta(t)}{dt} = \frac{2\kappa}{\tan \theta(t)} + \sqrt{2\kappa} \, \zeta_{\theta}(t);$$

$$r_0 \sin \theta(t) \frac{d\phi(t)}{dt} = \Omega r_0 \sin \theta(t) + \sqrt{2\kappa} \, \zeta_{\phi}(t), \tag{16}$$

where  $\kappa$  is the turbulent diffusivity of the magnetic footpoints on the source surface, which can be related to the Lagrangian

integral timescale  $\tau_L$  by

$$\kappa = \tau_L V_{\rm rms}^2 \tag{17}$$

Equation (17) is a direct consequence of Taylor's relation (6) at large time t. Taylor's relation is an exact result that connects the late-time asymptotics of the footpoint displacement variance to the Lagrangian autocorrelation function of the velocity field. We observe that Equation (17) is the definition of the diffusivity  $\kappa$  entering the Leighton (1964) model. Equation (17) is different from the expression  $\kappa \sim \lambda_c$  $V_{\rm rms}$ , where  $\lambda_c$  denotes the typical size of source surface convective structures, used by Leighton (1964) to describe the footpoint diffusivity. However, these two different expressions for the turbulent diffusivity coincide when  $\lambda_c = \tau_L V_{\rm rms}$ , corresponding to Kubo numbers on the order of unity. On the basis of the Leighton (1964) description of magnetic footpoint motions, Jokipii & Parker (1969) established a surface-driven model in which the stochastic magnetic field lines are obtained by expanding radially outward in the heliosphere, and at the solar wind speed, the trajectories of magnetic footpoints on the solar source surface. Assuming that the footpoint motions on the photosphere are Brownian, the boundary-driven stochastic Parker spirals in the solar wind are the solutions of the equations (Bian & Li 2021):

$$\frac{dr(t)}{dt} = V_{\text{sw}},$$

$$r_0 \frac{d\theta(t)}{dt} = \frac{2\kappa}{\tan \theta(t)} + \sqrt{2\kappa} \zeta_{\theta}(t),$$

$$r_0 \sin \theta(t) \frac{d\phi(t)}{dt} = \Omega r_0 \sin \theta(t) + \sqrt{2\kappa} \zeta_{\phi}(t).$$
(18)

The surface-driven magnetic field lines in the heliosphere are given by the curves  $[r(t), \phi(t), \theta(t)]$ , here parameterized by the time t it takes for a fluid parcel to travel a radial distance r. Because the magnetic field lines given by Equation (18) are not differentiable functions of t, their path lengths given by

$$L(r) = \int_0^{r/V_{\text{sw}}} dt \sqrt{V_{\text{sw}}^2 + r^2(t) \left(\frac{d\theta(t)}{dt}\right)^2 + r^2(t) \sin^2 \theta(t) \left(\frac{d\phi(t)}{dt}\right)^2},$$
(19)

are infinite for the  $d\theta(t)/dt$  and  $d\phi(t)/dt$  given by Equation (18). Furthermore, it is a well-known fact that the diffusion approximation contradicts Taylor's exact relation [Equation (6)] on timescales smaller than  $\tau_L$ . Based on these considerations, we have here extended the works of Leighton (1964) and Jokipii & Parker (1969) in order to develop a model consistent with smooth differentiable footpoint trajectories and hence smooth boundary-driven stochastic Parker spirals in the solar wind. The model is based on the spherical version of the Ornstein–Uhlenbeck process for the Lagrangian surface velocity, which, expressed in the heliographic coordinate system, results in boundary-driven magnetic field lines

described by the stochastic differential equations:

$$\frac{dr(t)}{dt} = V_{\text{sw}},$$

$$\frac{d\phi(t)}{dt} = \Omega + \frac{\delta V_{\phi}(t)}{r_0 \sin \theta(t)},$$

$$\frac{d\theta(t)}{dt} = \frac{\delta V_{\theta}(t)}{r_0},$$

$$\frac{d\delta V_{\theta}(t)}{dt} = -\frac{\delta V_{\theta}(t)}{\tau_L} + \delta V_{\phi}(t) \cos \theta(t)$$

$$\times \left(\Omega + \frac{\delta V_{\phi}(t)}{r_0 \sin \theta(t)}\right) + \sqrt{\frac{V_{\text{rms}}^2}{\tau_L}} \zeta_{\theta}(t),$$

$$\frac{d\delta V_{\phi}}{dt} = -\frac{\delta V_{\phi}(t)}{\tau_L} - \delta V_{\theta}(t) \cos \theta(t)$$

$$\times \left(\Omega + \frac{\delta V_{\phi}(t)}{r_0 \sin \theta(t)}\right) + \sqrt{\frac{V_{\text{rms}}^2}{\tau_L}} \zeta_{\phi}(t).$$
(20)

In this generalization of the Jokipii & Parker (1969) model, the path length L(r) given by Equation (19) is always bounded. The finite difference formulation of Equation (20), given by Equation (13), was integrated numerically to yield the magnetic footpoint trajectories illustrated in Figure 1 and the boundary-driven interplanetary magnetic field lines illustrated in Figure 2. The path-length distributions P(L, r=1 au) of magnetic field lines traced from the Sun to the Earth's orbit are also computed. These probability distribution functions are displayed for various values of the controlling parameters  $V_{\rm rms}$  and  $\tau_L$  in Figure 3.

Because the present Lagrangian stochastic model is a refined description of the Lagrangian velocity, which is the Eulerian velocity field evaluated along the fluid parcel trajectories, the typical size  $\lambda_c$  of the surface convective cells does not explicitly enter as a control parameter in the model, which is instead controlled by the Lagrangian integral timescale  $\tau_L$  in addition to  $V_{
m rms}$ . The Lagrangian integral timescale  $au_L$  is generally different from the Eulerian correlation timescale  $\tau_c$ . Nevertheless, Eulerian and Lagrangian parameters can be related for Kubo numbers on the order of unity. The present Lagrangian stochastic model differs from the Eulerian models (Giacalone 2001; Moradi & Li 2019), which rely on the assumption of incompressibility of the surface convective flows. It also offers substantial improvements over previous Lagrangian models (Leighton 1964; Jokipii & Parker 1969), which assume that the magnetic footpoint trajectories are Brownian motions yielding infinite path lengths of the magnetic field lines.

This work is supported in part by NASA grants 80NSSC21K1814, 80NSSC19K0075, and 80NSSC22K0268, and NSF ANSWERS grant 2149771 at UAH. Support by the ISSI and ISSI-BJ through International Team 469 is also acknowledged.

## ORCID iDs

Gang Li https://orcid.org/0000-0003-4695-8866 N. H. Bian https://orcid.org/0000-0003-0142-8669

#### References

```
Adhikari, L., Zank, G. P., & Zhao, L.-L. 2019, ApJ, 876, 26
Altschuler, M. D., & Newkirk, G. 1969, SoPh, 9, 131
Bian, N. H., & Li, G. 2021, ApJ, 908, 45
Bian, N. H., & Li, G. 2022a, ApJ, 924, 120
Bian, N. H., & Li, G. 2022b, ApJ, 941, 58
Cane, H. V., McGuire, R. E., & von Rosenvinge, T. T. 1986, ApJ, 301, 448
Chhiber, R., Matthaeus, W. H., Cohen, C. M. S., et al. 2021, A&A, 650, A26
Cohen, C. M. S., Mason, G. M., & Mewaldt, R. A. 2017, ApJ, 843, 132
Dalla, S., Balogh, A., Krucker, S., et al. 2003, GeoRL, 30, 8035
DeForest, C. E., Howard, T. A., & McComas, D. J. 2014, ApJ, 787, 124
Dresing, N., Gomez-Herrero, R., Heber, B., et al. 2014, A&A, 567, A27
Fan, C. Y., Pick, M., Pyle, R., Simpson, J. A., & Smith, D. R. 1968, JGR,
Giacalone, J. 2001, JGRA, 106, 15881
Giacalone, J., & Jokipii, J. R. 2004, ApJ, 616, 573
Gombosi, T. I., van der Holst, B., Manchester, W. B., & Sokolov, I. V. 2018,
   LRSP, 15, 4
Hathaway, D. H., Beck, J. G., Bogart, R. S., et al. 2000, AAS Meeting
  Abstract, 31, 05.04
Hathaway, D. H., Gilman, P. A., Harvey, J. W., et al. 1996, Sci, 272, 1306
Hathaway, D. H., & Rightmire, L. 2010, Sci, 327, 1350
Hathaway, D. H., Teil, T., Norton, A. A., & Kitiashvili, I. 2015, ApJ, 811, 105
Jokipii, J. R., & Parker, E. N. 1969, ApJ, 155, 777
Kahler, S., & Ragot, B. R. 2006, ApJ, 646, 634
Kelly, J., Dalla, S., & Laitinen, T. 2012, ApJ, 750, 47
Krucker, S., & Lin, R. P. 2000, ApJL, 542, L61
Lario, D., Kallenrode, M. B., Decker, R. B., et al. 2006, ApJ, 653, 1531
Leighton, R. B. 1964, ApJ, 140, 1547
Lin, R. P. 1974, SSRv, 16, 189
Lin, R. P., Potter, D. W., Gurnett, D. A., & Scarf, F. L. 1981, ApJ, 251, 364
Mewaldt, R. A., Cohen, C. M. S., Mason, G. M., et al. 2013, in AIP Conf. Ser.
   1539, Solar Wind 13, ed. G. P. Zank et al. (Melville, NY: AIP), 116
Moradi, A., & Li, G. 2019, ApJ, 887, 102
Parker, E. N. 1958, ApJ, 128, 664
Pei, C., Jokipii, J. R., & Giacalone, J. 2006, ApJ, 641, 1222
Reames, D. V. 1999, SSRv, 90, 413
Reames, D. V. 2009, ApJ, 706, 844
Reames, D. V., Ng, C. K., & Tylka, A. J. 2013, SoPh, 285, 233
Richardson, I. G., von Rosenvinge, T. T., Cane, H. V., et al. 2014, SoPh,
  289, 3059
Rincon, F., & Rieutord, M. 2018, LRSP, 15, 6
Rincon, F., Roudier, T., Schekochihin, A. A., & Rieutord, M. 2017, A&A,
Sáiz, A., Evenson, P., Ruffolo, D., & Bieber, J. W. 2005, ApJ, 626, 1131
Schatten, K. H., Wilcox, J. M., & Ness, N. F. 1969, SoPh, 6, 442
Schrijver, C. J., & DeRosa, M. L. 2003, SoPh, 212, 165
Shea, M. A., & Smart, D. F. 1990, SoPh, 127, 297
Tylka, A. J., Cohen, C. M. S., Dietrich, W. F., et al. 2003, ICRC (Tsukuba),
  6, 3305
Van Hollebeke, M. A. I., Ma Sung, L. S., & McDonald, F. B. 1975, SoPh,
Van Kooten, S. J., & Cranmer, S. R. 2017, ApJ, 850, 64
Wang, L., Krucker, S., Mason, G. M., Lin, R. P., & Li, G. 2016, A&A,
  585, A119
Wiedenbeck, M. E., Mason, G. M., Cohen, C. M. S., et al. 2013, ApJ, 762, 54
Zhang, M., McKibben, R. B., Lopate, C., et al. 2001, ICRC (Hamburg),
```

Zhang, M., McKibben, R. B., Lopate, C., et al. 2003, JGRA, 108, 1154

Zhao, L., Li, G., Zhang, M., et al. 2019, ApJ, 878, 107